# Geogrid-Aggregate Interlocking Mechanism Investigated via Discrete Element Modeling

Yu Qian, University of Illinois at Urbana-Champaign, USA, yuqian1@illinois.edu
Debakanta Mishra, University of Illinois at Urbana-Champaign, USA, dmishra2@illinois.edu
Hasan Kazmee, University of Illinois at Urbana-Champaign, USA, kazmee2@illinois.edu
Erol Tutumluer, University of Illinois at Urbana-Champaign, USA, tutumlue@illinois.edu

ABSTRACT
Geogrids provide reinforcement for aggregate materials through interlocking between granular particles and geogrid apertures. The reinforcement or stabilization effect of a geogrid can be quite different when used with similar aggregate types but having different particle size distributions. This paper describes recent research efforts at the University of Illinois focused on triaxial compression testing of pavement base course aggregate materials having different gradations. An aggregate image-aided numerical modeling approach based on the Discrete Element Method (DEM) was adopted in this study with the capability to create actual aggregate particles as three-dimensional polyhedron elements. The DEM simulations of aggregate assemblies then had the same grain size distributions and the imaging quantified average aggregate shapes and angularities. Cylindrical triaxial test specimens were simulated at two different gradations to investigate the geogrid-aggregate interlocking mechanism and how reinforcement benefits could be maximized. With higher coordination number, and therefore higher number of contacts between geogrid and aggregate particles, the specimen had a better packing structure, which yielded higher strength properties from the triaxial compression test.

## 1. INTRODUCTION

Geogrids have been successfully used for subgrade stabilization and base course reinforcement purposes in highway pavement applications. Geogrids can provide confinement and reinforcement to unbound aggregate layers due to their tensile strength and stiffness, and the interlocking between geogrid apertures and granular particles. The degree of interlocking between the geogrids and aggregates is controlled by many factors, i.e., aggregate size and shape properties, geogrid types and properties, compaction effort during installation, and loading conditions. To ensure effective interlocking between geogrids and aggregates, geogrids must be selected with appropriate aperture sizes to properly match with aggregate particle size distributions or gradations (Jewell et al. 1984). Previous studies have concluded for the same aggregate particle size distributions, reinforcement of geogrids with different aperture sizes can be quite different. McDowell et al. (2006) found a ratio of aperture size to particle diameter of about 1.4 gives optimum interlock based on a series of pull-out tests. Brown et al. (2007) performed cyclic plate loading tests and concluded for the 50 mm ballast used, the optimum aperture size was 60–80 mm. However, for typical dense-graded base course aggregate materials, the grain size distributions are more “well-graded” than ballast materials. The performance of geogrid reinforcement then varies considerably influenced by the interlocking mechanism (Kwon and Tutumluer 2009). Although several past lab and field studies have dealt with this topic, there is no clear conclusion about an optimal combination of geogrid aperture size and base course aggregate gradation. Further, no packing theory based aggregate gradation optimization approach has been studied to develop improved geogrid-aggregate interlocking mechanisms.

This paper describes preliminary findings from a research study recently initiated at the University of Illinois for developing a Discrete Element Method (DEM) based modeling approach which involves image analysis to realistically create actual aggregate particles as three-dimensional polyhedron elements having the same particle size distributions and imaging quantified average shapes and angularities. The DEM simulation approach has been successfully applied in simulating large-scale triaxial tests on ballast size aggregates with both biaxial and triangular aperture geogrids (Mishra et al. 2014). This paper investigates base layer aggregate gradation effects on the interlocking mechanisms by utilizing a commonly used geogrid with known properties. Triaxial compression tests are simulated using the DEM approach for various pavement base layer aggregate gradations having the same geogrid properties, i.e. aperture shape and size, to study packing arrangements and develop criteria using the packing theory variables, such as number of particle contacts, contact force magnitudes and coordination number, to improve geogrid reinforced aggregate base effectiveness so that higher shear strength and better resistance to settlement or permanent deformation can be achieved.

## 2. DESCRIPTION OF LABORATORY RAPID SHEAR TESTS

Tutumluer and Pan (2008) performed a series of laboratory triaxial compression tests to investigate the effect of aggregate morphology on strength and permanent deformation behavior of unbound aggregates. The aggregates were tested in dry (0% moisture content) condition with no fines (passing No. 200 sieve or less than 0.075 mm size) included

in the gradation. Each specimen was prepared 152 mm (6 in.) in diameter and 305 mm (12 in.) in height. Figure 1 shows the test equipment with a specimen after rapid shear test. The same void ratio of 67.5% was achieved for all triaxial rapid shear aggregate specimens by controlling the total volume of the aggregate particles contained in the specimen. The rapid shear test is a deformation controlled test with an axial strain of 12.5% (corresponding to 38 mm or 1.5 in.) obtained in 1 second at the confining pressure of 34.5 kPa (5 psi). Such a loading rate is reported to be highly effective in characterizing the bearing capacity failure of the unbound aggregate base/subbase layer under moving traffic loading (Garg and Thompson 1998). The aggregate shape properties including angularity index (AI) and surface texture (ST) index of those aggregate samples were quantified from three orthogonally acquired two-dimensional (2D) images of individual particles using the University of Illinois Aggregate Image Analyzer or UIAIA (Rao et al. 2002, Pan et al. 2006). Table 1 lists the properties of crushed limestone aggregate material and the rapid shear test results. The DEM simulation reproduced the triaxial compression test conducted on the crushed limestone as reported by Tutumluer and Pan (2008).

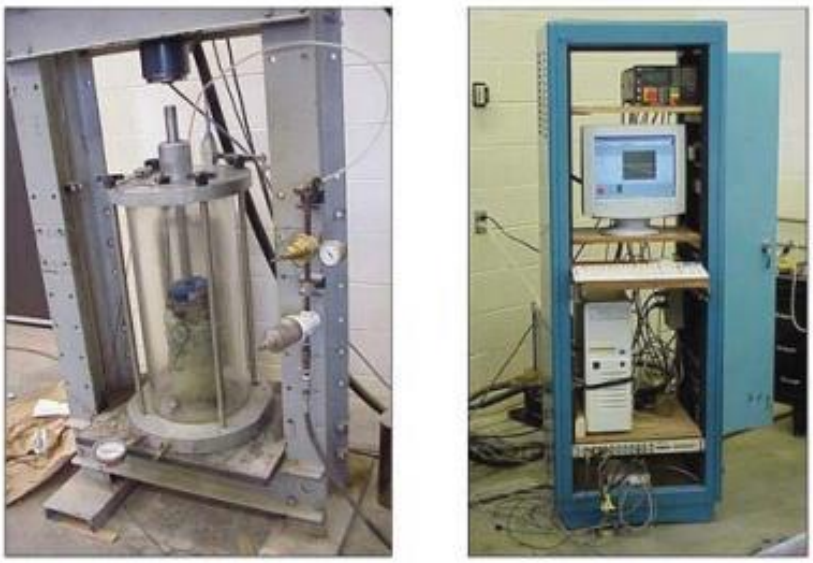

Figure 1. Servo-Hydraulic System and MTS 407 Controller Used for Rapid Shear Testing of Aggregate Specimens at the University of Illinois (Tutumluer and Pan, 2008; Mishra, 2012)

Table 1. Aggregate Properties and Rapid Shear Test Results

| Aggregate Type | Angularity Index (AI) | Surface Texture Index (ST) | Specific Gravity ($G_s$) | Specimen Weight (grams) | Max. Deviator stress $\sigma_d$ at Failure (kPa)[1] |
|---|---|---|---|---|---|
| Crushed Limestone | 495 | 1.75 | 2.735 | 9037 | 510 |

[1] Void ratio=67.5%; applied constant confining pressure $\sigma_3$=34.5 kPa (5 psi).

## 3. DESCRIPTION OF DISCRETE ELEMENT SIMULATIONS

### 3.1 Background: Image-aided DEM Capability

To investigate the mechanism of interlocking between aggregate particles and geogrid apertures and how this minimizes particle movement and causes local stiffness increase through friction and interaction of ballast particles with geogrid, a numerical modeling approach was adopted based on the Discrete Element Method (DEM) combined with image analyses of tested aggregate particles for size and shape properties. Compared to other research studies focusing on simulating triaxial tests by DEM, which often use spherical elements or element clusters (Indraratna et al. 2010, Lu and McDowell 2010), the image-aided DEM simulation approach developed at the University of Illinois has the capability to create actual ballast aggregate particles as three-dimensional polyhedron elements having the same particle size distributions and imaging quantified average shapes and angularities. Ghaboussi and Barbosa (1990) developed the first polyhedral 3D DEM code BLOKS3D for particle flow; and Nezami et al. (2006) enhanced the program with new, fast

contact detection algorithms. Tutumluer et al. (2006) combined the DEM program and the aggregate image analysis together to simulate the aggregate behavior more accurately and realistically by using polyhedral elements regenerated from the image analysis results of ballast materials. This DEM approach was first calibrated by laboratory large scale direct shear test results for ballast size aggregate application (Huang and Tutumluer 2011). The calibrated DEM model was then utilized to model strength and settlement behavior of railroad ballast for the effects of multi-scale aggregate morphological properties (Tutumluer et al. 2006, 2007). More recent applications of the calibrated DEM model investigated ballast gradation (Tutumluer et al. 2009) and fouling issues (Tutumluer et al. 2008, Huang and Tutumluer 2011) that are known to influence track performance. A successful field validation study was also conducted with the ballast DEM simulation approach through constructing and monitoring field settlement records of four different ballast test sections and then comparing the measured ballast settlements under monitored train loadings to DEM model predictions (Tutumluer et al. 2011). The effects of geogrid aperture shape and geogrid location in a triaxial test specimen were recently studied by this DEM approach (Qian et al. 2011, Mishra et al. 2014).

## 3.2 Development of DEM Simulations

### 3.2.1 Aggregate and geogrid in DEM simulations

To investigate effects of base layer aggregate gradations on the interlocking mechanisms by utilizing a commonly used geogrid with known properties, different pavement base layer aggregate gradations having the same imaging based particle shape indices, i.e. angularity index (AI), flat and elongated ratio (F&E), and surface texture index (SI), were selected. The first gradation used in the laboratory rapid shear test, Gradation 1, was considered as the original gradation for validation purposes. Another gradation, Gradation 2, was next created by changing the percentage passing of certain sieve sizes. Note that changing the percentage passing of certain sieve may or may not change the particle packing and mechanical behavior of the granular assembly significantly without changing the specimen density (Boler et al. 2014). Figure 2 presents the two gradations used in the DEM simulations. Gradation 1 was the same as the gradation used in laboratory rapid shear test (Pan and Tutumluer, 2008). Gradation 2 changed the passing 19 mm sieve to 76% (from the previous 96%) while the percentage passing values of the other sieves remained the same as Gradation 1. Aggregate particles were generated in DEM simulations according to the grain size distributions shown in Figure 2 and the average imaging based shape indices listed in Table 1. Figure 3 shows the geogrid used in the DEM simulations. The geogrid was simulated by joining rigid bar elements together for making the square shaped apertures. The aperture size was 39 mm by 39 mm, similar to common geogrid available in the market.

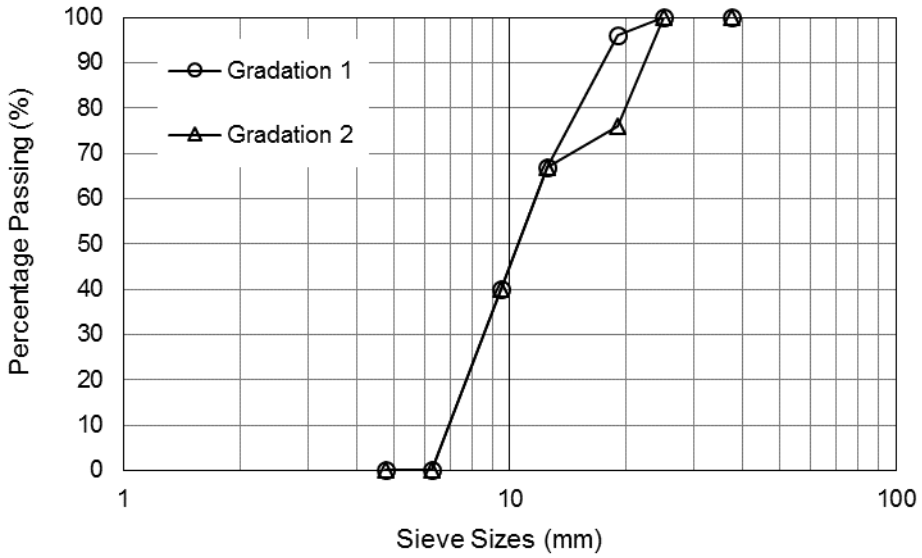


Figure 2. Particle size distributions of crushed limestone aggregate used in DEM test simulations

### 3.2.2 Flexible membrane in DEM test simulations

Lee et al. (2012) recently used rigid rectangular cuboid discrete elements positioned in a cylindrical arrangement to simulate a flexible membrane with BLOKS3D. A similar approach was used in this study. To avoid a long run-time, the

incremental shearing scheme reported elsewhere is adopted herein to reproduce the shearing process (Lee et al. 2012, Qian et al. 2013). A total of 240 rectangular cuboid discrete elements (in ten-layers) were used to form a cylindrical chamber to confine the aggregate specimen. Each layer had 24 equal size elements and the dimension of each single element was 203.2 mm (4 in.) long, 101.6 mm (2 in.) wide, and 30.5 mm (1.2 in.) high. These membrane elements were only allowed translational movement in radial direction. Rotation and translation movements in other directions were restricted to replicate the deformation of membrane. Other details of using rigid cuboid discrete elements to simulate flexible membrane behavior can be found elsewhere (Lee et al. 2012, Qian et al. 2013).

### 3.2.3 DEM test simulation procedures

After the flexible membrane was formed, around 2,000 particles were poured into the cylinder to create the unreinforced aggregate specimen. Then, the top platen was placed on top to compact the specimen to the same initial density under 34.5 kPa (5 psi) confining pressure as achieved in the laboratory experiment. Figure 4 presents the DEM model preparation procedures. For the geogrid reinforced specimens, after the membrane was formed, about 2,000 particles were also poured into the cylinder in two different sets (1,000 particles for each set) following the same gradation and shape properties of the aggregates particles used in the laboratory (see Figure 4a). In between, a sheet of geogrid element was placed in the middle of the specimen as shown in Figure 4b and the upper part of the specimen was generated next (see Figure 4c). The simulated geogrid has a square aperture shape with an opening size of 39 mm. The bar element in the geogrid has thickness of 2.3 mm and depth of 1.0 mm. When the specimen in the DEM simulation was prepared in a similar condition with the laboratory test specimen, i.e., density, initial voids and geometry, extra particles were removed from the top and the triaxial compression shear test was started using the "incremental displacement shearing method" (Lee et al. 2012, Qian et al. 2013) until desired axial strain was achieved.

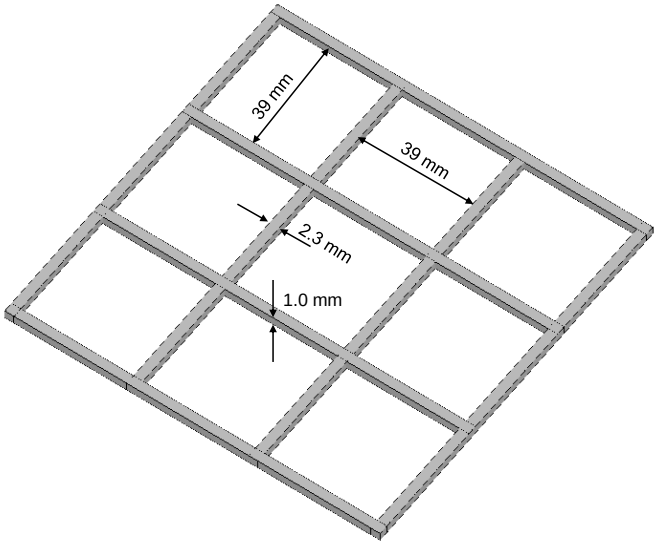


Figure 3. Geogrid element used in DEM test simulations

### 3.2.4 DEM test simulation results

Figure 5 presents the results of the DEM triaxial strength test simulations on the crushed limestone cylindrical specimens with and without geogrid reinforcement for up to 10% axial strain. The maximum deviator stresses at failure obtained for each specimen are summarized in Table 2. Note that the peak deviator stress achieved from the laboratory triaxial compression test was 510 kPa, as listed in Table 1. In comparison, the peak deviator stress for the specimen with Gradation 1, without geogrid reinforcement, was computed to be 552 kPa, fairly close to the experimental result. Based on the DEM test simulations, the stress-strain curves of the different gradation specimens are also generated and plotted for comparison in Figure 5. Gradation 2 which had 76% percent particles passing 19 mm sieve has more large particles and has a more "well-graded" gradation when compared to Gradation 1, which had 96% percent particles passing 19 mm sieve and most the particles were falling into the range of 12.5 mm to 6.25 mm sizes. Although there were only 1,201 particles, specimen with Gradation 2 generated much higher strength than specimen with Gradation 1, which had 1,860 particles. The peak deviator stress obtained from simulation for Gradation 1 and Gradation 2, both without geogrid reinforcement, were 552 kPa and 734 kPa, respectively.

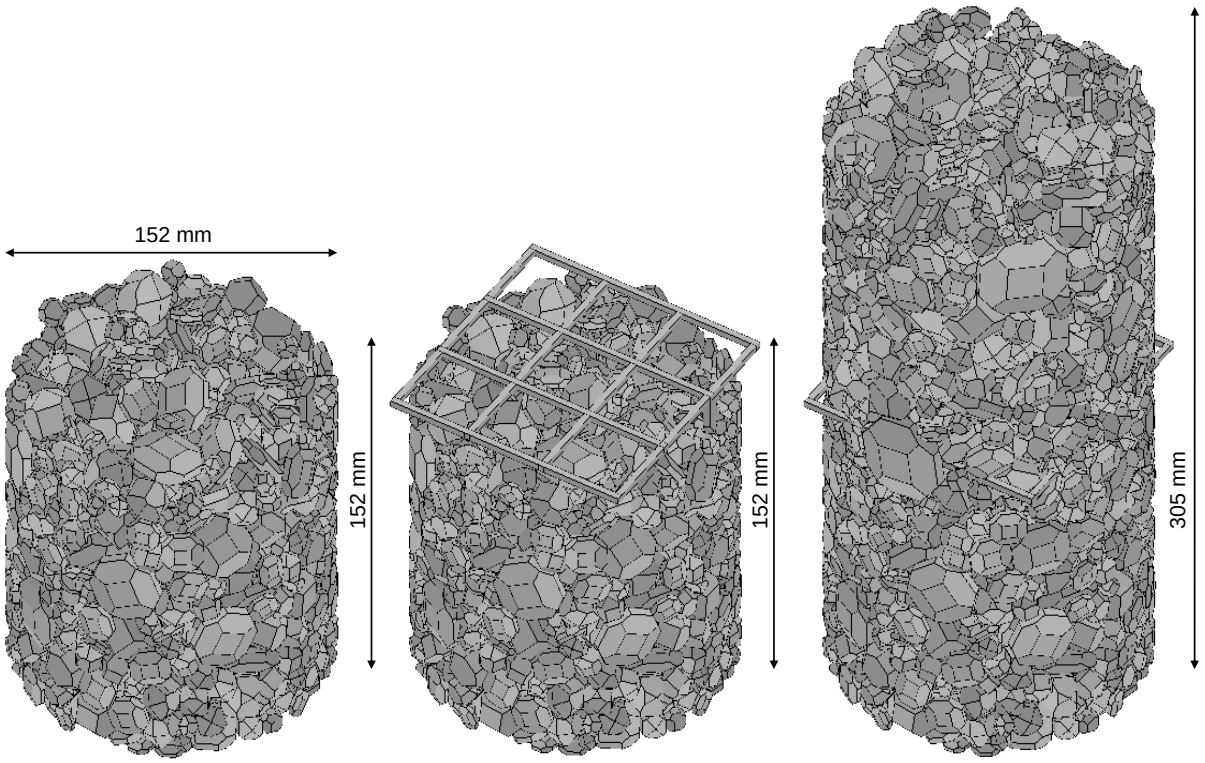


(a) Generate bottom particles (b) Generate geogrid sheet (c) Generate top particles

Figure 4. Geogrid-reinforced sample preparation procedures for the DEM test simulations

Table 2. DEM Test Simulation Results for Each Specimen

| Specimen | Gradation 1 | | Gradation 2 | |
|---|---|---|---|---|
| | Unreinforced | Reinforced | Unreinforced | Reinforced |
| Peak Deviator stress (kPa) | 552 | 649 | 734 | 812 |
| Strength Benefit | 17.6% | | 11.6% | |
| No. of Particles (Elements) | 1,860 | 1,867 | 1,201 | 1,196 |
| Average* Coordination Number | 2.48 | 2.48 | 3.29 | 3.28 |
| Average* No. of Contacts for the geogrid | -- | 39.4 | -- | 26.3 |

*During shearing stage

Simulations with different gradations and geogrid reinforcement included showed similar stress-strain behavior at the initial small strain stage of the strength tests for up to 2% axial strain; this was primarily due to the fact that geogrids were not yet fully mobilized early on. When axial strain levels increased, the geogrid was mobilized and the interlock between geogrid and aggregate particles prevented movement or specimen bulging. The zigzag shapes of the stress-strain curves at high axial strain levels indicate sudden strength drops or peaks. The geogrid reinforcement simulation in this study showed the geogrid effectively increased the strength of aggregate specimens during triaxial compression testing.

The peak deviator stresses for geogrid-reinforced specimens of Gradation 1 and Gradation 2 were 649 kPa and 812 kPa, respectively. As listed in Table 2, the peak deviator stresses increased about 17.6% and 11.6% respectively due to the geogrid reinforcement.

Another advantage of DEM test simulations is that all the contacts between particles can be tracked and recorded for each time step throughout the simulation. Therefore, the coordination number, which is defined as the average number of contacts that one particle makes with its neighbors, can be tracked to indicate the packing structure of the aggregate specimen (Gu and Yang, 2013). It was reported that a higher coordinate number would result in better performance of aggregates (Boler et al. 2014).

Accordingly, Table 2 gives the coordination numbers averaged throughout the entire compression stage in DEM test simulations for different gradations. Specimen with Gradation 1 had an average coordination number of 2.48 while specimen with Gradation 2 had an average coordination number of 3.29. The average coordination number results indicate that particles in specimen with Gradation 2 had higher number of contacts with their neighboring particles, which probably caused a better packing structure to sustain higher deviator stresses during shearing. The contact between the geogrid and aggregate particles could also be tracked and recorded throughout the DEM test simulations. Table 2 also lists the average number of contacts between the geogrid sheet and the aggregate particles; 39.4 for the specimen with Gradation 1 and 26.3 for the specimen with Gradation 2. Effective contacts between the geogrid sheet and the DEM particles/elements can prevent lateral movement or rotation of particles thus reducing specimen bulging and increasing specimen shear strength. Furthermore, the average number of contacts between the geogrid and the aggregate particles can qualitatively represent how well the geogrid can arrest aggregate particles. With higher number of contacts between the geogrid and the particles in specimen of Gradation 1, the peak deviator stress increased by 17.6%.

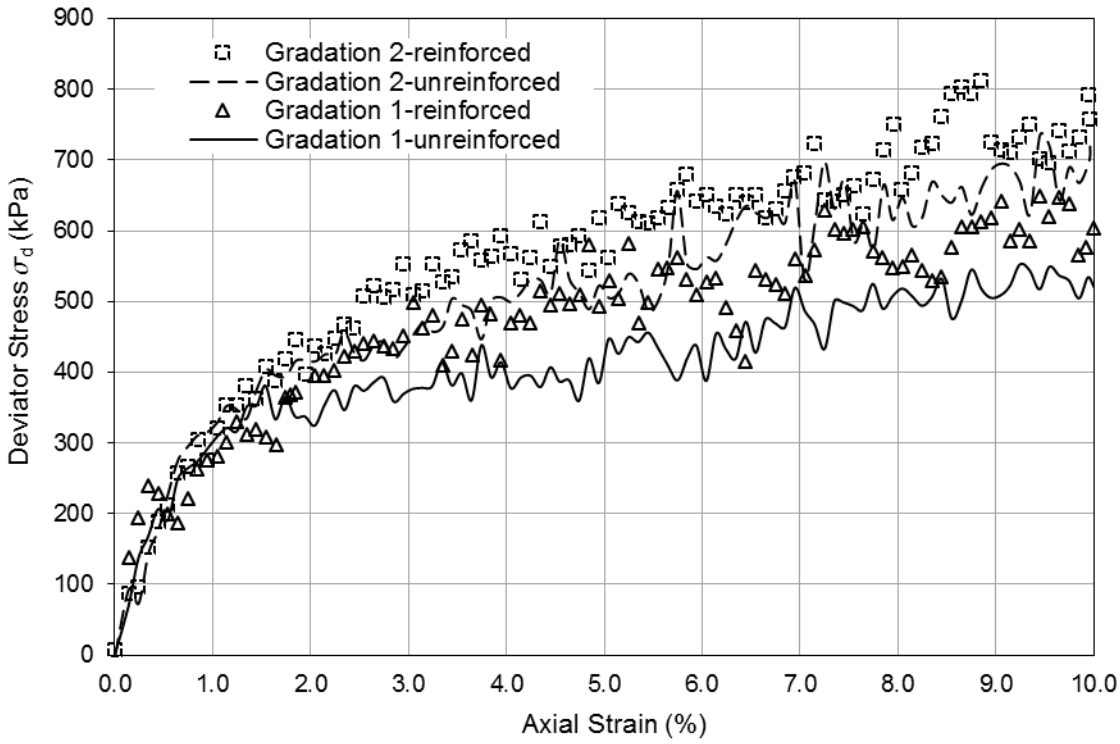


Figure 5. Stress-strain Curves Generated from the DEM Triaxial Compression Strength Test Simulations

## 4. DISCUSSION

This paper focused on an investigation of slightly different aggregate gradations affecting the geogrid-aggregate interlocking mechanisms studied through triaxial compression tests. Numerical simulations were carried out based on the Discrete Element Method (DEM) modeling approach, which also involved image analysis based quantifications of aggregate particle size and shape properties. Laboratory triaxial compression tests were simulated using the DEM modeling approach to study shear strength responses of specimens prepared at two different gradations and with and without geogrid reinforcement. The goal was to demonstrate the applicability of the aggregate image-aided DEM

simulation platform for evaluating packing theory based micromechanical interactions of different sized aggregate particles interlocking with the geogrid and as a result, establishing a technique to quantify improved geogrid reinforcement benefits. Based on the preliminary testing and DEM simulation results with limited data, the following conclusions can be drawn from this study:

1. The DEM simulation approach developed at the University of Illinois has the capability to simulate triaxial compression tests performed on base course aggregate materials with or without geogrid reinforcement. The DEM simulation approach has the ability to quantify important micromechanical interactions through packing theory variables, such as number of contacts between geogrid and aggregate particles and specimen coordination number, which are quite difficult to record during actual laboratory experiments.
2. Aggregate specimens with different gradations can have quite different strength and deformation characteristics. With a higher coordination number, specimens had a better packing structure, which yielded higher strength during DEM triaxial compression test simulations.
3. Geogrid reinforcement effect depends on aggregate gradation and geogrid aperture size. With more effective contact between geogrid and aggregate particles, the geogrid-aggregate interlocking based reinforcement or stabilization effect can be better pronounced.
4. The DEM simulation platform, currently being further developed, has the potential to be a quantitative tool to predict the improved aggregate-geogrid interactions. This methodology has the potential for optimizing the selection of geogrid products for aggregate materials with different gradations. Further, this methodology also has the potential to improve geogrid product development for specific target applications.

REFERENCES


Boler, H., Qian, Y., Tutumluer, E. (2014). Statistical Analyses of Railroad Ballast Aggregate Packing Influenced by Changes in Gradation and Particle Shape Properties. Accepted by *Transportation Research Record: Journal of the Transportation Research Board*, Transportation Research Board of the National Academies, Washington, D.C.

Brown, S. F., Kwan, J. and Thom, N. H. (2007). Identifying the Key Parameters that Influence Geogrid Reinforcement of Railway Ballast. *Geotextiles and Geomembranes*, 25(6):326-335.

Garg, N. and Thompson, M.R. (1997). Triaxial Characterization of Minnesota Road Research Project Granular Materials. *Transportation Research Record* No. 1577: 27-36.

Ghaboussi J. and Barbosa R. (1990). Three-dimensional Discrete Element Method for Granular Materials. *International Journal for Numerical and Analytical Methods in Geomechanics*, (14): 451-472.

Gu, X.Q. and Yang, J. (2013). A Discrete Element Analysis of Elastic Properties of Granular Materials. *Granular Matter*, 15(2): 139-147.

Huang H., and Tutumluer E. (2011). Discrete Element Modeling for Fouled Railroad Ballast. *Construction and Building Materials*, (25): 3306–3312.

Indraratna, B., Thakur, P.K., and Vinod, J.S. (2010). Experimental and Numerical Study of Railway Ballast Behavior under Cyclic Loading. *International Journal of Geomechanics*, ASCE, 10(4):136-144.

Jewell, R.A., Milligan, G.W.E., Sarsby, R.W. and Dubois, D. (1984). Interaction between Soil and Geogrids. Proceedings of the Symposium on Polymer Grid Reinforcement in Civil Engineering, London, U.K., 1984, pp. 19–29.

Kwon, J. and Tutumluer, E. (2009). Geogrid Base Reinforcement with Aggregate Interlock and Modeling of the Associated Stiffness Enhancement in Mechanistic Pavement Analysis. *Transportation Research Record No. 2116*, National Research Council, Washington, D.C.:85-95.

Lee, S. J., Hashash, Y.M.A., and Nezami E.G. (2012). Simulation of Triaxial Compression Test with Polyhedral Discrete Elements. *Computers and Geotechnics*, 43:92-100.

Lu, M. and McDowell, G.R. (2010). Discrete Element Modelling of Railway Ballast under Monotonic and Cyclic Triaxial Loading. *Geotechnique*, 60(6):459-467.

McDowell, G.R., Harireche, O., Konietzky, H., Brown, S.F., and Thom, N.H. (2006). Discrete Element Modelling of Geogrid-Reinforced Aggregates. *In Proceedings of the Institution of Civil Engineers—Geotechnical Engineering*, 159: 35-48.

Mishra, D. (2012). Aggregate Characteristics Affecting Response and Performance of Unsurfaced Pavements on Weak Subgrades. Ph.D. Dissertation, University of Illinois at Urbana-Champaign.

Mishra, D., Qian, Y., Kazmee, H., Tutumluer, E. (2014). Investigation of Geogrid-Reinforced Railroad Ballast Behavior Using Large-Scale Triaxial Testing and Discrete Element Modeling. Accepted by *Transportation Research Record: Journal of the Transportation Research Board*, Transportation Research Board of the National Academies, Washington, D.C.

Nezami E.G., Hashash, Y.M.A., Zhao D., Ghaboussi J. (2006). Shortest Link Method for Contact Detection in Discrete Element Method. *International Journal for Numerical and Analytical Methods in Geomechanics*, 30(8):783-801.

Pan, T., Tutumluer, E., and Carpenter, S.H. (2006). Effect of Coarse Aggregate Morphology on Permanent Deformation Behavior of Hot Mix Asphalt. *Journal of Transportation Engineering*, 132(7): 580-589.

Qian, Y., Tutumluer, E., and Huang, H. (2011). A Validated Discrete Element Modeling Approach for Studying Geogrid-Aggregate Reinforcement Mechanisms. *Geo-Frontiers 2011*, ASCE Geo-Institute, March 13-16, Dallas, Texas.

Qian, Y., Lee, S., Tutumluer, E., Hashash, Y.M.A., Mishra, D., and Ghaboussi, J. (2013). Discrete Element Method for Simulating Ballast Shear Strength from Large Triaxial Tests. *Transportation Research Record* No. 2374: 126-135.

Rao, C., Tutumluer, E. and Kim, I.T. (2002). Quantification of Coarse Aggregate Angularity Based on Image Analysis. *Transportation Research Record*. No. 1787, 193-201.

Tutumluer, E., and Pan, T. (2008). Aggregate Morphology Affecting Strength and Permanent Deformation Behavior of Unbound Aggregate Materials. *Journal of Materials in Civil Engineering*, 20(9):617–627.

Tutumluer, E., Huang, H., Hashash, Y.M.A., and Ghaboussi, J. (2006). Aggregate Shape Effects on Ballast Tamping and Railroad Track Lateral Stability. *In Proceedings of the AREMA Annual Conference*, Louisville, Kentucky, USA, September 17-20.

Tutumluer, E., Huang, H., Hashash, Y.M.A., and Ghaboussi, J. (2007). Discrete Element Modeling of Railroad Ballast Settlement. *In Proceedings of the AREMA Annual Conference*, Chicago, Illinois, September 9-12.

Tutumluer, E., Huang, H., Hashash, Y.M.A., and Ghaboussi, J. (2009). AREMA Gradations Affecting Ballast Performance Using Discrete Element Modeling (DEM) Approach. *In Proceedings of the AREMA Annual Conference*, Chicago, Illinois, September 20-23.

Tutumluer, E., Qian, Y., Hashash, Y.M.A., Ghaboussi, J., and Davis, D.D. (2013). Discrete Element Modelling of Ballasted Track Deformation Behaviour. *International Journal of Rail Transportation*, 1(1-2): 57-73.